AIP | Applied Physics Letters

Influence of hydrogen on the structure and stability of ultra-thin ZnO on metal substrates

Bjoern Bieniek, Oliver T. Hofmann, and Patrick Rinke

Citation: Applied Physics Letters **106**, 131602 (2015); doi: 10.1063/1.4917015
View online: http://dx.doi.org/10.1063/1.4917015
View Table of Contents: http://scitation.aip.org/content/aip/journal/apl/106/13?ver=pdfcov
Published by the AIP Publishing

Influence of hydrogen on the structure and stability of ultra-thin ZnO on metal substrates

Bjoern Bieniek,[1] Oliver T. Hofmann,[1,2] and Patrick Rinke[1,3,a)]
[1]*Fritz-Haber-Institut der Max-Planck-Gesellschaft, 14195 Berlin, Germany*
[2]*Institut für Festkörperphysik, TU Graz, 8010 Graz, Austria*
[3]*School of Science, Aalto University, FI-00076 Aalto, Finland*

(Received 3 February 2015; accepted 26 March 2015; published online 3 April 2015)

We investigate the atomic and electronic structure of ultra-thin ZnO films (1 to 4 layers) on the (111) surfaces of Ag, Cu, Pd, Pt, Ni, and Rh by means of density-functional theory. The ZnO monolayer is found to adopt an α-BN structure on the metal substrates with coincidence structures in good agreement with experiment. Thicker ZnO layers change into a wurtzite structure. The films exhibit a strong corrugation, which can be smoothed by hydrogen (H) adsorption. An H over-layer with 50% coverage is formed at chemical potentials that range from low to ultra-high vacuum H_2 pressures. For the Ag substrate, both α-BN and wurtzite ZnO films are accessible in this pressure range, while for Cu, Pd, Pt, Rh, and Ni wurtzite films are favored. The surface structure and the density of states of these H passivated ZnO thin films agree well with those of the bulk $ZnO(000\bar{1}) - 2 \times 1 - H$ surface. © *2015 AIP Publishing LLC*.
[http://dx.doi.org/10.1063/1.4917015]

In the context of hybrid inorganic/organic systems, ZnO is a common inorganic component for optoelectronic devices.[1–4] However, the structure of the polar $(000\bar{1})$ and (0001) surfaces, which is often used in these hybrid systems, is under heavy debate,[5–10] hampering further quantitative interface studies. Another important application of ZnO lies in the field of heterogeneous catalysis. In industrial catalytic processes, ZnO supported metal nanoparticles are frequently used to convert syngas.[11]

In both cases, metal supported ultra-thin oxide films have been proposed as model systems to understand the interface structure and its chemistry, because they facilitate the application of the standard tool set of surface science, such as photoelectron spectroscopy and scanning tunneling microscopy, and prevent charging effects. However, some ultra-thin films exhibit their own interesting properties,[12–15] which differ from bulk materials. For example, the formation of a graphitic ZnO_x species was suggested and experimentally observed in the vicinity of nano-particles.[16,17] It is thus not clear to what degree ultra-thin metal-supported ZnO films resemble the surfaces of ZnO or whether they exhibit significantly different properties.

To answer this question and to characterize ultra-thin metal supported ZnO films, we have performed density-functional theory (DFT) calculations for 1 to 4 layers films on various metal substrates. We focus in this paper on one geometrical property, the corrugation of the surface, and one electronic property, the density of states, and compare them to the bulk ZnO surface. Furthermore, we address the differences in the atomic structure and thermodynamic stability of pristine and H-covered ultra-thin ZnO films on the transition metals: Ag, Cu, Pd, Pt, Ni, and Rh. Other aspects that determine the similarity of metal supported ultra-thin ZnO films to bulk ZnO polar surfaces are the formation energies and charge transition levels of common defects,[18] the associated position of the films' or surfaces' Fermi level,[19,20] and the role of the image effect induced by the metal substrate. These will be investigated in future work.

We use DFT as implemented in the FHI-aims code[21] together with the Perdew-Burke-Ernzerhof (PBE) functional[22] and a Monkhorst-Pack[23] k-grid of 15 × 15 × 15 k-points in the primitive unit-cell. We simulate surfaces as periodically repeated slabs. To compensate the artificial electrostatic field due to the asymmetric slab geometry, we apply a dipole correction.[24] ZnO films on metal substrates are initialized in an ideal α-BN structure. The geometry of the ZnO and the two metal layers closest to the interface is relaxed until the forces are below 0.05 eV/Å per atom. Long range van-der-Waals forces were accounted for by the Tkatchenko-Scheffler (TS)-scheme[25] with parameters adapted to surface and polarization effects.[26,27] The parameters are listed in the supplementary material (SI[28]). For the smallest structures (i.e., ultra-thin ZnO on Cu) the PBE functional was tested against the higher level Heyd-Scuseria-Ernzerhof (HSE06) hybrid functional.[29] The changes in relaxed geometries are small and the main difference in the density of states is the larger ZnO band gap (see SI[28]).

The starting point for our investigations are hypothetical free-standing ZnO films without a metal substrate. They adopt an α-BN structure in analogy to graphene.[30–33] To obtain a stable combination of metal and ZnO mono-layer, we have to address the lattice mismatch between the two constituents. Too much strain will force the film out of its preferred planar structure towards a wurtzite-like structure.[34] According to our calculations (see Fig. 1), the switch from planar to wurtzite occurs at a ZnO in-plane lattice parameter of 3 Å (∼9% strain). The strain in the films can be minimized by tuning the coincidence to match the in-plane lattice parameter of the ZnO ultra-thin films on metals with the lattice parameter of the free-standing mono-layer ZnO. We

a)Electronic mail: patrick.rinke@aalto.fi

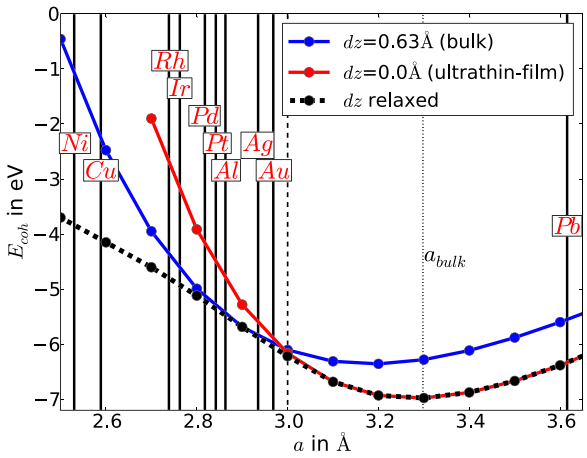

FIG. 1. Cohesive energy E_{coh} of an ideal α-BN (dz = 0 Å), a wurtzite/zinc-blend (dz = 0.63 Å), and a relaxed ZnO mono-layer as a function of the in-plane lattice parameter a. The in plane lattice parameters $(a/\sqrt{2})$ of the (111) surface of selected fcc transition metals are indicated by vertical lines.

confirmed this observation by considering the formation energy ΔH of the combined system (ZnO mono-layer on the metal) as a function of the number of unit-cells m along the in-plane lattice vectors of the metal

$$\Delta H = (E_{Tot} - m^2 E_M - (m-1)^2 E_{ZnO})/A, \qquad (1)$$

with the total energy of the coincidence slab E_{Tot}, the energy of the 1×1 metal surface E_M, the energy of the free-standing 1×1 ZnO mono-layer E_{ZnO}, and the surface area of the structure A. For $m \times m$ metal unit cells with a fixed lattice parameter a_M, this results in $(m-1) \times (m-1)$ unit-cells of ZnO with a ZnO lattice parameter of $a_{ZnO} = \frac{m-1}{m} \frac{a_M}{\sqrt{2}}$. The results are shown in Table I. The agreement with experimental values for sub-monolayer ZnO islands is good (Ag,[35,36] Pd,[37] Pt,[38] Au,[39] Cu (brass),[40] and Ru (0001)[41]). The coincidence structures for which the ZnO in-plane lattice parameter is closest to that of the free-standing structure gives the lowest formation energy. The theoretically predicted coincidence structure depends on the relation between the metal and ZnO lattice parameters obtained with a specific xc-functional. For larger coincidence structures (Ag, Pd, Pt), small changes in the lattice parameters can lead to a different predicted coincidence structure, while systems with small coincidence structures (Ni, Cu) are less sensitive (see SI[28] for a comparisons of different xc-functionals). To distinguish

TABLE I. Experimental and calculated coincidence structures (m × m-1) for ZnO mono-layers on the (111) surface of different transition metals. dz is the corrugation of the ZnO mono-layer and the strain is the lattice mismatch between adsorbate film and free-standing mono-layer. dz is 0.63 Å for ideal bulk wurtzite and 0 Å for an ideal free-standing ZnO α-BN mono-layer. ΔΦ is the work function change between the bare metal surface and the ZnO mono-layer on the metal substrate.

Metal	Strain (%)	Coincidence	Experimental	ΔΦ (eV)	dz (Å)
Ag	0.7	9 × 8	8 × 7[a]	0.14	0.127
Pd	0.8	7 × 6	6 × 5[b]	0.06	0.237
Pt	0.2	7 × 6	6 × 5[c]	−0.04	0.246
Ni	1.0	4 × 3	…	−0.05	0.266
Cu	−2.0	5 × 4	…	0.43	0.292
Rh	0.8	6 × 5	…	0.07	0.337

[a]References 35 and 36.
[b]Reference 37.
[c]Reference 38.

between the α-BN and wurtzite structure, we define the corrugation dz as the mean distance of the oxygen atoms from the plane spanned by its three surrounding Zn atoms. By this definition, dz would be 0 Å for ideal α-BN and 0.63 Å for wurtzite ZnO. The corrugation dz (Table I) of the film does not correlate with the lattice mismatch between metal and film. The free-standing monolayer would not exhibit any corrugation within the range of residual strains observed for ZnO on the metal substrates (see Fig. 1). We attribute the larger corrugation of ZnO on Cu, Rh, Pd, and Pt to chemical effects such as a larger affinity for oxygen and thus a prevalence for oxide formation and the different distances between surface metal atoms and ZnO due to the varying size of the coincidence structures.

With growing number of ZnO layers on the metal substrates, the corrugation of the ZnO ultra-thin films increases. Strain in the ZnO films (Cu, Ni, Pd) facilitates the formation of a bulk-like wurtzite structure. We will restrict our investigations to the O-terminated multi-layer ZnO films on the metal substrates and investigate their stability with respect to a residual H atmosphere. A more detailed analysis of both terminations including the influence of OH and other reconstruction is deferred to future work.

The phase diagrams for different coverages of H on ZnO ultra-thin films on different metals as function of the number of ZnO layers are now analyzed by *ab initio* atomistic thermodynamics.[42,43] We consider the surface free energy γ

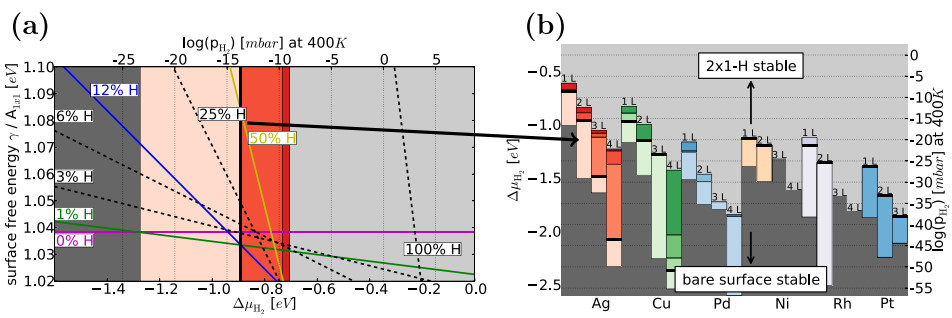

FIG. 2. (a) Surface free energy γ per (1×1) Ag surface unit-cell area as a function of the change in chemical potential $\Delta\mu$ (see Eq. (2)) for 2 layers (8×8) ZnO on $(9 \times 9 \times 4)$ Ag with different coverages of H. The partial pressure, as calculated from thermodynamical tables, of H_2 at 400 K is plotted in the top axis. The red area indicates the transition region between the ultra-thin film without H (dark gray) and the 2×1–H with 50% H coverage (light gray). (b) The three different regimes corresponding to the dark gray, colored, and light gray areas in (a) for different metals and different numbers of ZnO layers (L).

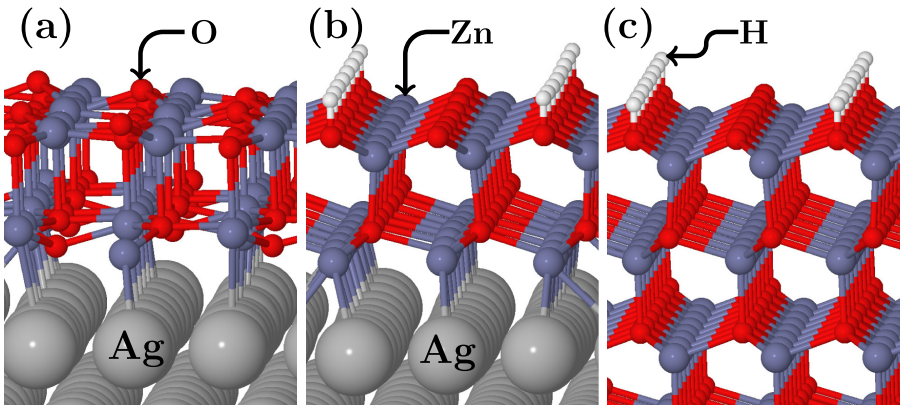

FIG. 3. (a) Structure of (8 × 8 × 2) ZnO on (9 × 9 × 4) Ag without H adsorption. (b) (8 × 8 × 2) ZnO on (9 × 9 × 4) Ag surface slab with 50% H coverage. (c) Zn0$(000\bar{1})-2\times1$–H surface. Only parts of the unit-cells are shown.

$$\gamma(T,p_{\mathrm{H}}) = \frac{1}{A}\left[E^{tot} + F^{vib} - TS^{conf} + pV - N_{\mathrm{M}}E^{bulk}_{\mathrm{M}} - N_{\mathrm{ZnO}}E^{bulk}_{\mathrm{ZnO}} - N_{\mathrm{H}}\Delta\mu_{\mathrm{H}}(T,p_{\mathrm{H}})\right] \quad (2)$$

as a function of the change of the H chemical potential, $\Delta\mu = \mu_H - E_{H_2}/2$. E^{tot} is the total energy of the slab-calculation, N_{M}, N_{ZnO}, N_{H} are the number of the respective species, and E_{M}, E^{bulk}_{ZnO}, $E_{\mathrm{H_2}}$ are the reference energies of their bulk or molecular forms, obtained with the PBE + vdW xc-functional (see SI[28]). F^{vib} is the vibrational free energy, S^{conf} is the configurational entropy, p is the total pressure, and V is the total volume. The impact of these three contributions on the surface phase diagrams can be found in the literature[43] and in detail for ZnO on metal substrates in the SI.[28] The pV-term can be safely neglected. The effect on the 2 × 1–H reconstruction is less pronounced due to the steep inclination (N_{H}/surface sites) of its stability line in the phase diagram (Fig. 2(a)). In Fig. 2 and for the further discussion vdW-effects, S^{conf} and F^{vib} are taken into account.

The chemical potential is translated into partial pressures for a given, exemplary temperature (400 K) with the help of the ideal gas law and thermodynamic tables.[44] Our calculations show that the bulk terminated ZnO surface is only stable for low H_2 partial pressures. At elevated chemical potentials of H_2, the 2 × 1–H structure becomes the most stable surface (see Figs. 3(b) and 2). Disordered H distributions, H at the interface, and H adsorbed at the Zn-sites are higher in energy (see SI[28]). With increasing H termination, the films become more and more wurtzite-like and the surface adopts the 2 × 1–H structure. For all calculated systems, the partial pressure region for the transition from the clean (α-BN) film to the 2 × 1–H reconstruction is shown in Fig. 2(b). Below the colored bars (dark gray regions, lower pressures), the graphite-like films are stable, above (light gray region, higher pressures) 2 × 1–H is stabilized. In the region marked by the bars, H-coverages larger than 0% and smaller than 50% are stable. H coverages corresponding to one H per unit cell (determined by the coincidence structure) dominate this transition regime. Our results show that for Ag at 400 K the clean surface as well as the 2 × 1–H reconstruction could be realized experimentally for layer numbers greater than 2. Thus, the H_2 partial pressure can be used to select one of the two phases. For Cu and Ni, the structure without H and the intermediate H-coverages are reachable only at elevated temperatures. For Pd and Rh, only the 2 × 1–H reconstruction is within experimentally accessible pressure ranges. For increased H pressures, the difference in the formation energies between systems with different numbers of ZnO layers is significantly reduced (see SI[28]). Under experimental conditions, some of these structures could be kinetically stabilized and further growth be hindered.[38] The formation of the 2 × 1–H reconstruction, though thermodynamically most stable, could be blocked by an energy barrier for the dissociation of H_2 at the surface.

Finally, we address the electronic structure. The comparison of the density of states for the 2 × 1–H reconstructed ZnO $(000\bar{1})$ surface and the ZnO films on the metals in Fig. 4 shows that systems with 4 and more layers already resemble the 2 × 1–H reconstructed ZnO $(000\bar{1})$ surface very well. The films without H retain a unique character. The electronic structure differs from the ZnO $(000\bar{1})$–2 × 1–H surface and the geometry combines aspects of wurtzite and α-BN.

In summary, we have shown stable coincidence structures for bulk-terminated ZnO thin films on Ag, Cu, Pd, Ni, Pt, and Rh. The mono-layers exhibit a graphene-like α-BN structure with a pronounced corrugation depending on the

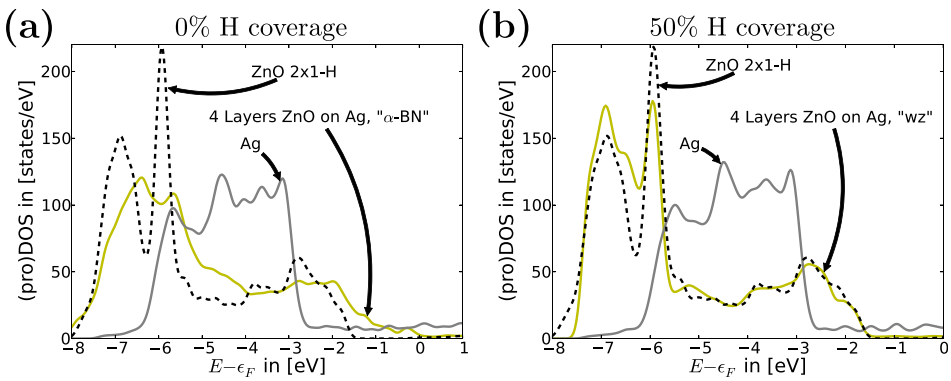

FIG. 4. (a) Comparison of projected DOS of 4 Layers (8 × 8) ZnO on (9 × 9 × 4) Ag without H and (b) with 50% H coverage with the DOS of a ZnO 2 × 1–H surface slab. The projected DOS of the ZnO 2 × 1–H surface is shifted by −1 eV in (a) and (b) with respect to their Fermi level.

lattice mismatch with the substrate. With increasing number of ZnO layers, the α-BN structure destabilizes. For increased H_2 partial pressures, the atomic and electronic structure resembles that of bulk terminated ZnO $(000\bar{1})$–2×1–H (see Fig. 3(c)), whereas at low H_2 partial pressures H-free graphitic ultra-thin films are stable. The choice of metal and the H_2 partial pressure are therefore two additional degrees of freedom to select between ultra-thin ZnO films, which differ from bulk ZnO, and films that resemble wurtzite ZnO and could serve as important models for the study of the ZnO $(000\bar{1})$–2×1–H surface.

The authors thank Matthias Scheffler, Shamil Shaikhutdinov, and Takashi Kumagai for fruitful discussions in the process of this work. This work was supported by the Deutsche Forschungsgemeinschaft DFG through the collaborative research project 951 "HIOS," by the Austrian Science Fund FWF through the Erwin-Schrödinger Grant No. J 3258-N20 and by the Academy of Finland through its Centers of Excellence Program (#251748).

[1]M. Law, L. E. Greene, J. C. Johnson, R. Saykally, and P. Yang, Nat. Mater. **4**, 455 (2005).
[2]Y. Yang, G. A. Turnbull, and I. D. W. Samuel, Appl. Phys. Lett. **92**, 163306 (2008).
[3]M. Sessolo and H. J. Bolink, Adv. Mater. **23**, 1829 (2011).
[4]J. W. Levell, M. E. Giardini, and I. D. W. Samuel, Opt. Express **18**, 3219 (2010).
[5]G. Kresse, O. Dulub, and U. Diebold, Phys. Rev. B **68**, 245409 (2003).
[6]B. Meyer, Phys. Rev. B **69**, 045416 (2004).
[7]C. Wöll, Prog. Surf. Sci. **82**, 55 (2007).
[8]M. Valtiner, M. Todorova, and J. Neugebauer, Phys. Rev. B **82**, 165418 (2010).
[9]J. V. Lauritsen, S. Porsgaard, M. K. Rasmussen, M. C. R. Jensen, R. Bechstein, K. Meinander, B. S. Clausen, S. Helveg, R. Wahl, G. Kresse, and F. Besenbacher, ACS Nano **5**, 5987 (2011).
[10]R. Wahl, J. V. Lauritsen, F. Besenbacher, and G. Kresse, Phys. Rev. B **87**, 085313 (2013).
[11]M. Behrens, F. Studt, I. Kasatkin, S. Kühl, M. Hävecker, F. Abild-Pedersen, S. Zander, F. Girgsdies, P. Kurr, B.-L. Kniep, M. Tovar, R. W. Fischer, J. K. Norskov, and R. Schlögl, Science **336**, 893 (2012).
[12]C. Freysoldt, P. Rinke, and M. Scheffler, Phys. Rev. Lett. **99**, 086101 (2007).
[13]G. Pacchioni, Chemistry **18**, 10144 (2012).
[14]S. Shaikhutdinov and H.-J. Freund, Annu. Rev. Phys. Chem. **63**, 619 (2012).
[15]C. Noguera and J. Goniakowski, Chem. Rev. **113**, 4073 (2013).
[16]R. Naumann d'Alnoncourt, X. Xia, J. Strunk, E. Loffler, O. Hinrichsen, and M. Muhler, Phys. Chem. Chem. Phys. **8**, 1525 (2006).
[17]S. Zander, E. L. Kunkes, M. E. Schuster, J. Schumann, G. Weinberg, D. Teschner, N. Jacobsen, R. Schlögl, and M. Behrens, Angew. Chem., Int. Ed. **52**, 6536 (2013).
[18]A. Janotti and C. G. V. de Walle, Rep. Prog. Phys. **72**, 126501 (2009).
[19]N. A. Richter, S. Sicolo, S. V. Levchenko, J. Sauer, and M. Scheffler, Phys. Rev. Lett. **111**, 045502 (2013).
[20]Y. Xu, O. T. Hofmann, R. Schlesinger, S. Winkler, J. Frisch, J. Niederhausen, A. Vollmer, S. Blumstengel, F. Henneberger, N. Koch, P. Rinke, and M. Scheffler, Phys. Rev. Lett. **111**, 226802 (2013).
[21]V. Blum, R. Gehrke, F. Hanke, P. Havu, V. Havu, X. Ren, K. Reuter, and M. Scheffler, Comput. Phys. Commun. **180**, 2175 (2009).
[22]J. P. Perdew, K. Burke, and M. Ernzerhof, Phys. Rev. Lett. **77**, 3865 (1996).
[23]H. J. Monkhorst and J. D. Pack, Phys. Rev. B **13**, 5188 (1976).
[24]L. Bengtsson, Phys. Rev. B **59**, 12301 (1999).
[25]A. Tkatchenko and M. Scheffler, Phys. Rev. Lett. **102**, 073005 (2009).
[26]G.-X. Zhang, A. Tkatchenko, J. Paier, H. Appel, and M. Scheffler, Phys. Rev. Lett. **107**, 245501 (2011).
[27]V. G. Ruiz, W. Liu, E. Zojer, M. Scheffler, and A. Tkatchenko, Phys. Rev. Lett. **108**, 146103 (2012).
[28]See supplementary material at http://dx.doi.org/10.1063/1.4917015 for lattice parameters, coincidence structures for different xc-functionals, a comparison to results obtained with HSE06, interfacial hydrogen, DFT atomic structures, and the influence of vibrational free energy and configurational entropy.
[29]J. Heyd, G. E. Scuseria, and M. Ernzerhof, J. Chem. Phys. **118**, 8207 (2003).
[30]F. Claeyssens, C. L. Freeman, N. L. Allan, Y. Sun, M. N. R. Ashfold, and J. H. Harding, J. Mater. Chem. **15**, 139 (2005).
[31]C. L. Freeman, F. Claeyssens, N. L. Allan, and J. H. Harding, Phys. Rev. Lett. **96**, 066102 (2006).
[32]Z. C. Tu and X. Hu, Phys. Rev. B **74**, 035434 (2006).
[33]M. Topsakal, S. Cahangirov, E. Bekaroglu, and S. Ciraci, Phys. Rev. B **80**, 235119 (2009).
[34]D. Wu, M. G. Lagally, and F. Liu, Phys. Rev. Lett. **107**, 236101 (2011).
[35]C. Tusche, H. L. Meyerheim, and J. Kirschner, Phys. Rev. Lett. **99**, 026102 (2007).
[36]A. Shiotari, B. H. Liu, S. Jaekel, L. Grill, S. Shaikhutdinov, H.-J. Freund, M. Wolf, and T. Kumagai, J. Phys. Chem. C **118**, 27428 (2014).
[37]G. Weirum, G. Barcaro, A. Fortunelli, F. Weber, R. Schennach, S. Surnev, and F. P. Netzer, J. Phys. Chem. C **114**, 15432 (2010).
[38]Y. Martynova, B.-H. Liu, M. McBriarty, I. Groot, M. Bedzyk, S. Shaikhutdinov, and H.-J. Freund, J. Catal. **301**, 227 (2013).
[39]X. Deng, K. Yao, K. Sun, W.-X. Li, J. Lee, and C. Matranga, J. Phys. Chem. C **117**, 11211 (2013).
[40]V. Schott, H. Oberhofer, A. Birkner, M. Xu, Y. Wang, M. Muhler, K. Reuter, and C. Wöll, Angew. Chem., Int. Ed. **52**, 11925 (2013).
[41]D. Kato, T. Matsui, and J. Yuhara, Surf. Sci. **604**, 1283 (2010).
[42]M. Scheffler and J. Dabrowski, Philos. Mag. A **58**, 107 (1988).
[43]K. Reuter, C. Stampfl, and M. Scheffler, *Handbook of Materials Modeling*, edited by S. Yip (Springer, Berlin, Heidelberg, 2005), pp. 149–194.
[44]M. W. J. Chase, *NIST-JANAF Thermochemical Tables*, 4th ed. (American Institute of Physics, New York, 1998).